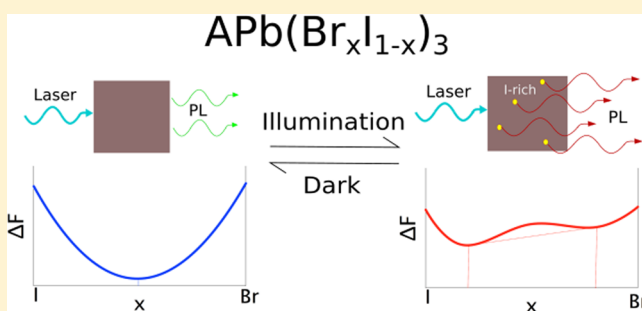


Light-Induced Phase Segregation in Halide-Perovskite Absorbers

Daniel J. Slotcavage,[†] Hemamala I. Karunadasa,^{*,‡} and Michael D. McGehee^{*,†,Ⓜ}[†]Department of Materials Science and Engineering, Stanford University, 476 Lomita Mall, Stanford, California 94305, United States[‡]Department of Chemistry, Stanford University, 337 Campus Drive, Stanford, California 94305, United States

ABSTRACT: In the few short years since the inception of single-junction perovskite solar cells, their efficiencies have skyrocketed. Perovskite absorbers have at least as much to offer tandem solar cells as they do for single-junction cells due in large part to their tunable band gaps. However, modifying the perovskite band structure via halide substitution, the method that has been most effective at tuning band gaps, leads to instabilities in the material for some compositions. Here, we discuss the thermodynamic origin and consequences of light-induced phase segregation observed in mixed-halide perovskites. We propose that, as the phase segregation is rooted in halide migration and possibly affected by lattice strain, modifying the perovskite composition and lattice structure, increasing compositional uniformity, and reducing defect concentrations could significantly improve stability.



Perovskite solar cells have progressed faster than any other solar cell technology to date. In the few short years since Kojima et al. first showed that hybrid perovskites function as solar absorber materials,¹ research in the characterization and optimization of perovskite materials and devices has exploded. Their high defect tolerance,^{2–4} sharp absorption onsets,⁵ long carrier diffusion lengths,⁶ and low surface recombination velocities⁷ make hybrid perovskites ideal candidates for absorbers/emitters in solar cells or LEDs.^{8,9} Already single-junction hybrid perovskite solar cell efficiencies exceed 21%,¹⁰ and the efficiencies for devices using a variety of perovskites continue to grow steadily.^{11–13} While single-junction solar cells have been extremely successful, there has also been a significant push to use high-band-gap perovskites as the top absorber in tandem solar cells with Si, CIGS, or low-band-gap perovskites.^{14–22}

Ideally, the top cell of a perovskite/Si monolithic tandem should have a band gap of 1.7–1.8 eV.²³ Unfortunately for tandems, most of the highest-performing perovskites have band gaps around 1.5–1.6 eV.^{10–12,24} Significant work has been invested in creating higher-band-gap perovskite absorbers, mostly by interchanging bromide and iodide in the X site (where the perovskite is of the form ABX₃). While replacing iodide with bromide does increase the band gap for the perovskites studied for solar applications, Noh et al. showed that for MAPb(Br_xI_{1-x})₃, this increase in band gap does not yield a corresponding increase in open-circuit voltage.²⁵ Hoke et al. showed that mixed I/Br perovskites underperform because of light-induced halide phase segregation (referred to from here onward as the Hoke effect) that leads to the formation of smaller-

band-gap “trap” states.²⁶ Since the discovery of the Hoke effect, many groups have worked to understand the system’s underlying electronic processes, model its thermodynamics, and develop more stable materials to prevent it.

In this Perspective, we review experimental observations of the Hoke effect in mixed-halide perovskite absorbers. We discuss existing thermodynamic models, generated and tested through simulations that fit the data, and analyze their agreement with experimental results. Finally, we examine the work that has been performed as well as future pathways for development of mixed-halide perovskites that eliminate the Hoke effect for solar-relevant illumination intensities.

Experimental Observations. Several groups have demonstrated that substituting Br for I in the MAPbI₃ lattice monotonically increases the material’s band gap.^{25,27} However, when incorporated into solar cells, these higher-band-gap materials did not exhibit the higher open-circuit voltages that we would expect when increasing the band gap. In fact, solar cells made with mixed-halide perovskites containing more than 20% bromide (MAPb(Br_xI_{1-x})₃; $x > 0.2$) actually showed a decrease in open-circuit voltage with increasing bromide content.²⁵ Hoke et al. further investigated and discovered that interchanging X-site halides introduces an inherent instability in the material.²⁶ Measuring both the initial photoluminescence (PL, Figure 1a) and the absorption of MAPb(Br_xI_{1-x})₃ showed the expected monotonic increase in band gap from 1.6 to 2.3 eV with

Received: September 30, 2016

Accepted: November 7, 2016

Published: November 7, 2016

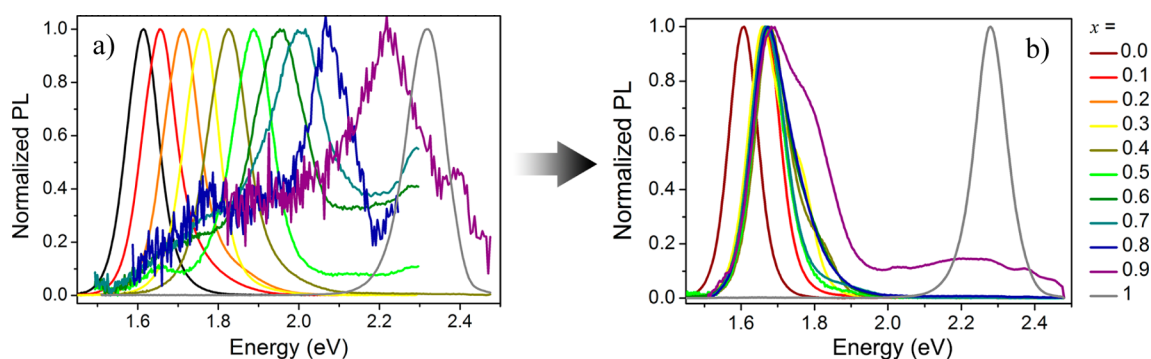


Figure 1. Normalized PL spectra of MAPb(Br_xI_{1-x})₃ thin films before (a) and after (b) illuminating for 5–10 min with 10–100 mW cm⁻² (~1–10 suns), 457 nm light. Reproduced from ref 26 with permission from The Royal Society of Chemistry.

increasing bromide content. However, the PL evolved in time. For materials with $x > 0.2$, the initial PL intensity slowly decreased while a new, lower-energy peak developed with much higher intensity, as shown in Figure 1b. Measuring this effect for a range of Br/I ratios revealed both that this new peak forms at almost the same energy for all compositions in the range $0.2 \leq x < 1$ and that this energy corresponds to the initial (and final) PL peak energy of the $x = 0.2$ member of the series (Figure 1b). They hypothesized that bromide and iodide ions phase segregated upon illumination into higher-band-gap Br-rich and lower-band-gap I-rich domains. The relatively long lifetimes and carrier diffusion lengths in perovskites^{6,28,29} suggest that photo-generated carriers would sample a significant volume fraction of the lattice before radiatively recombining. During diffusion, carriers have ample opportunity to survey multiple crystallographic domains and should rapidly thermalize and become trapped upon encountering any I-rich low-band-gap region. The change in band structure between an I-rich domain and the uniformly mixed perovskite could also generate an electric field that might further aid in sweeping carriers into the I-rich domain. Thus, nearly all of the PL should come from the radiative relaxation of carriers trapped in I-rich regions, consistent with the results of PL measurements. Figure 2 shows a qualitative depiction of the band gaps of the original mixed-halide, I-rich, and Br-rich perovskite phases. In our lab, the observation that

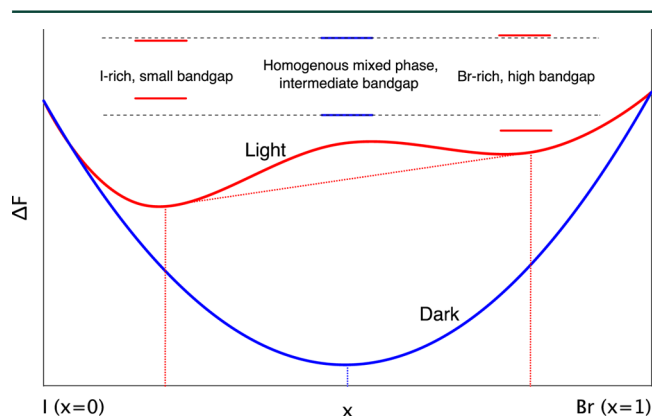


Figure 2. Schematic Helmholtz free-energy curves in the light and in the dark predicting phase segregation and energy diagram sketches of the relative band gaps of each phase. The red dashed lines show that the lowest attainable free energy in the light occurs when the material segregates into I-rich and Br-rich phases, while the blue dashed line shows that the lowest energy is attained when the material remains in a single phase in the dark.

halides phase segregate was the first indication that halides moved significantly in MAPb(Br_xI_{1-x})₃ and led us to hypothesize that halide migration and J – V hysteresis in solar cells could be linked. That other halide perovskites and related metal halides are known to be halide conductors^{30–33} further corroborates the idea that halides in this system could be mobile. Recent transient absorption measurements support our proposals that phase segregation occurs and that carriers quickly relax into the “trap” state by showing transient bleaches of both a high-band-gap and low-band-gap phase.³⁴ Their results demonstrate that once excited carriers have driven phase segregation rapid thermalization of those carriers from the higher band gap to the new, lower-energy state occurs on the picosecond time scale.

The observation that halides phase segregate was the first indication that halides moved significantly in MAPb(Br_xI_{1-x})₃ and led us to hypothesize that halide migration and J – V hysteresis in solar cells could be linked.

To look for structural changes caused by phase segregation, Hoke et al. measured X-ray diffraction (XRD) patterns of MAPb(Br_xI_{1-x})₃ films with and without illumination. When illuminated with white light, the sharp reflections of the original diffraction pattern split into two peaks, suggesting the formation of phases with a larger and a smaller lattice constant (Figure 3). This is consistent with halide segregation as the iodide-rich phase should have a larger lattice constant than the bromide-rich phase. Even more interestingly, when allowed to relax in the dark, the XRD pattern returned to its original, single-phase state. PL and absorption spectra taken before and after light soaking both confirmed this reversibility and demonstrated that the material can be repeatedly cycled between its segregated and unsegregated states without any signs of degradation. Bischak et al. employed cathodoluminescence both to confirm the existence of this phase segregation and to pinpoint its spatial location and found that I-rich clusters form at grain boundaries.³⁵

Finally, to confirm that the Hoke effect occurs due to illumination and not from sample heating during illumination, Hoke et al. performed PL measurements over a range of temperatures. They found that the disappearance of the original peak and corresponding rise of the lower-energy peak occurred even at low temperatures. The time scale of the change, however, varied significantly; at room temperature, the change occurred in about 1 min, but at 200 K, the new peak took almost 1 h to

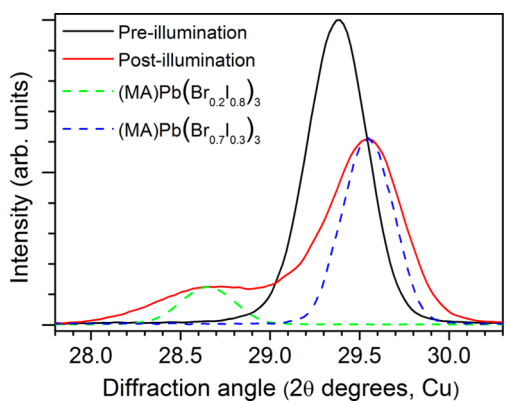


Figure 3. The 200 XRD peak of an $x = 0.6$ film before (black) and after (red) white-light soaking for 5 min at 50 mW cm^{-2} ($\sim 1/2$ sun). XRD patterns of an $x = 0.2$ film (dashed green) and an $x = 0.7$ film (dashed blue) are included for comparison. Reproduced from ref 26 with permission from The Royal Society of Chemistry.

dominate the original peak at $\sim 1/10$ sun intensity. Importantly, they held the excitation density constant through these measurements as they observed that the rates of growth of the new peak and disappearance of the original peak depended strongly on illumination intensity. Plotting the initial growth rate of the new peak as a function of temperature demonstrated that the phase segregation follows Arrhenius behavior. The activation energy calculated is similar to halide conductivity activation energies for other halide perovskites and related metal halides^{30–33} (Figure 4 inset). Finding similar values for the

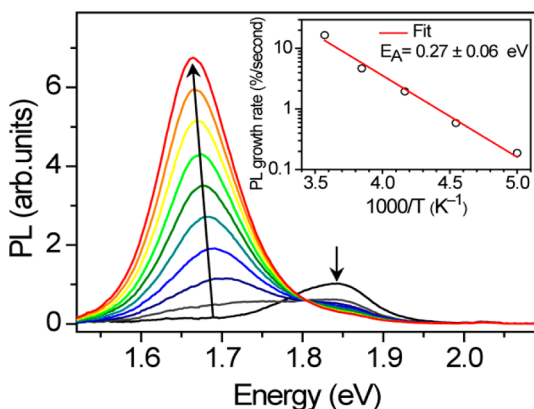


Figure 4. PL spectra of a $\text{MAPb}(\text{Br}_{0.4}\text{I}_{0.6})_3$ thin film over 45 s in 5 s increments under 457 nm , 15 mW cm^{-2} ($\sim 1/10$ sun) light at 300 K. (Inset) Temperature dependence of the initial PL growth rate. Reproduced from ref 26 with permission from The Royal Society of Chemistry.

activation energy for phase segregation in $\text{MAPb}(\text{Br}_x\text{I}_{1-x})_3$ and for activation energies of halide transport in related metal halides reaffirms the proposal that halides phase segregate and further supports the now common belief that ionic transport processes play a significant role in perovskite solar cell device physics.

Thermodynamics of the Hoke Effect. Interested in the thermodynamic origin of the Hoke effect, Brivio et al. employed density functional theory (DFT) to study the solid solution $\text{MAPb}(\text{Br}_x\text{I}_{1-x})_3$.³⁶ They calculated the system's Helmholtz free energy as a function of halide composition and temperature and found a miscibility gap at room temperature. This behavior suggests that, should the system receive sufficient energy to

kinetically overcome its metastable uniform mixed-halide state, the material will phase segregate into I-rich and Br-rich phases. They suggest that illumination provides the necessary energy to overcome the kinetic barriers trapping the material in its metastable state, causing it to phase segregate. However, while this theory successfully shows that the Hoke effect should occur at room temperature, it does not explain the reversibility observed previously. Their phase diagram predicts that once phase segregated the phases should be closer to thermodynamic equilibrium. The material should therefore remain phase segregated upon the removal of illumination, which is inconsistent with previous experimental data showing the reversibility of the Hoke effect.

Opting for molecular dynamics simulations to investigate the thermodynamics of the Hoke effect, Bischak et al. attempted to explain the difference in free energy of $\text{MAPb}(\text{Br}_x\text{I}_{1-x})_3$ in the light and in the dark.³⁵ Their findings show that when absorbed light generates an electron–hole pair, the pair quickly dissociates. Due to the ionic nature of the perovskite, the free electron and hole deform the surrounding lattice through electron–phonon coupling. Such polaronic behavior has been previously shown both experimentally and computationally for MAPbI_3 .^{37–39} Bischak et al. suggest that for $\text{MAPb}(\text{Br}_x\text{I}_{1-x})_3$ this carrier-induced lattice distortion increases the magnitude of the enthalpy of mixing enough to change the shape of the free energy versus bromine content curve from one that has only one minimum (the blue curve in Figure 2) to one that has two minima (the red curve in Figure 2). Their model suggests that small, naturally occurring fluctuations in perovskite composition that exist prior to illumination yield I-rich regions with reduced band gaps. Upon illumination, generated polarons funnel into the reduced-band-gap I-rich domains. The concentrated polaron density near I-rich domains creates a substantial change in free energy curves between the light and dark states, driving the perovskite to form I-rich and Br-rich phases with final compositions dictated by the system's free energy. Consequentially, any source of compositional nonuniformity will encourage phase segregation, and conversely, uniformity will encourage stability. When allowed to relax in the dark, the perovskite's free energy returns to its preillumination state and it becomes energetically favorable to form a single phase once again. Using our XRD data of mixed-halide perovskite films under illumination, we previously found that the halide-segregated nanometer-scale domains experienced anisotropic strain disorder and proposed that this, along with entropy, may assist the material's homogenization in the dark.²⁶

Material Design. An improved understanding of the thermodynamics governing $\text{MAPb}(\text{Br}_x\text{I}_{1-x})_3$ introduces oppor-

An improved understanding of the thermodynamics governing $\text{MAPb}(\text{Br}_x\text{I}_{1-x})_3$ introduces opportunities to mitigate the Hoke effect for high-band-gap mixed-halide perovskites.

tunities to mitigate the Hoke effect for high-band-gap mixed-halide perovskites. So far, morphological enhancements,⁴⁰ compositional tuning,^{41,42} and external pressure⁴³ have all been shown to reduce or effectively eliminate the Hoke effect in a variety of perovskites.

Several groups have demonstrated that morphological improvements can significantly improve stability to the Hoke

effect. The Hoke effect depends upon diffusion of Br and I within the perovskite. Similar to other metal halides,⁴⁴ halide migration in perovskites is thought to occur through halogen vacancies,⁴⁵ and ion mobility in these materials is known to be more facile at grain boundaries compared to that of the bulk material.⁴⁶ Therefore, reducing the defect density and the number of grain boundaries should decrease the rate at which phase segregation occurs. In order to obtain higher-quality films with larger grains and lower defect densities that should limit the Hoke effect, Hu et al. applied their method of solution processing perovskite films toward mixed I/Br systems.⁴⁰ As they anticipated, enhanced crystallinity and larger grain sizes showed a reduction in both the XRD peak splitting and PL peak red shifting associated with the Hoke effect. Sutter-Fella et al. observed similar stabilization with improvements in film quality.⁴⁷ Notably, these results demonstrate that, for a given composition, morphology can play a significant role in a film's susceptibility to the Hoke effect. Their work suggests that, with some optimization, materials previously deemed unstable to phase segregation may be kinetically stable toward phase segregation for solar-relevant operating conditions.

With some optimization, materials previously deemed unstable to phase segregation may be kinetically stable toward phase segregation for solar-relevant operating conditions.

Compositional tuning complements morphological improvement as a method for limiting the Hoke effect. On the basis of results showing strong electron–phonon coupling in MA perovskites,^{35,39} Bischak et al. predict that modifying perovskite composition reduces the lattice distortion caused by excited carriers. Reducing these lattice distortions should promote thermodynamic favoring of the uniform phase, limiting the Hoke effect. Specifically, they suggest that the perovskite can be stabilized by replacing MA with formamidinium (FA) or Cs. This theory agrees with earlier results from Beal et al. and McMeekin et al. as these groups have created more stable perovskites with Cs (Figure 5) and Cs/FA blends, respectively.^{41,42} For example, Beal et al. report phase stability with up to 40% Br in $\text{CsPb}(\text{Br}_x\text{I}_{1-x})_3$ at 1 sun illumination, significantly better than

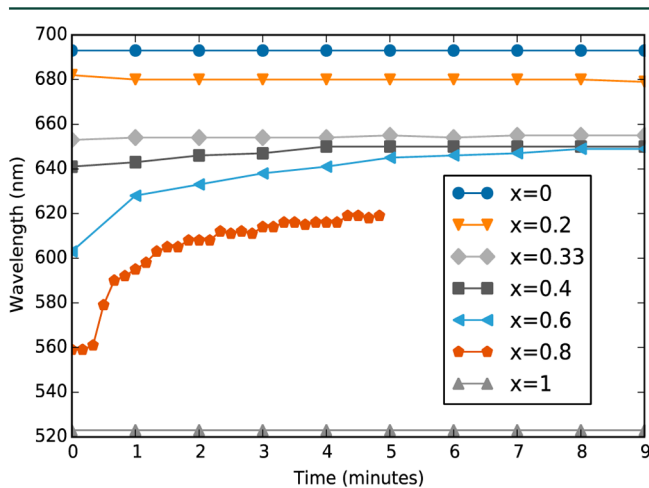


Figure 5. PL peak position as a function of time for $\text{CsPb}(\text{Br}_x\text{I}_{1-x})_3$ materials under ~ 1 sun illumination. Reproduced from ref 42.

the stability up to 20% Br reported by Hoke et al. for $\text{MAPb}(\text{Br}_{0.2}\text{I}_{0.8})_3$. McMeekin et al. also report improved stability for $\text{Cs}_{0.17}\text{FA}_{0.83}\text{Pb}(\text{Br}_{0.4}\text{I}_{0.6})_3$ when compared to its MA analogue (excited at $\sim 1/30$ sun). These results demonstrate that certain perovskites appear to be less susceptible to the Hoke effect than the prototypical MA mixed-halide perovskites and that simply tuning the perovskite's composition may entirely eliminate the Hoke effect at solar-relevant intensities. Given that compositional tuning to limit the Hoke effect has been limited to only a few substitutions at the perovskite A site, significant room for innovation still exists in this space. It should be noted, however, that neither of these studies controlled the morphology when claiming improved stability to the Hoke effect. This makes decoupling any potential morphology-induced improvements from the benefits of changing the cation difficult, and future studies should consider this point carefully when evaluating stability.

Rather than modifying the composition or film morphology to reduce the Hoke effect, Jaffe et al. instead tested the effects of material compression to thermodynamically or kinetically suppress halide migration.⁴³ They realized that by applying external pressure, they may change the equilibrium defect concentration. As halides are believed to diffuse via vacancies in hybrid perovskites,^{45,48,49} external pressure could thus affect halide diffusion. Lattice stiffness may also change the dynamics of halide migration. Measuring the PL of $\text{MAPb}(\text{Br}_{0.6}\text{I}_{0.4})_3$ powder in a diamond-anvil cell indeed revealed that as the pressure increased the degree of phase segregation decreased. From 0 to 0.8 GPa, the compressed material showed the Hoke effect. However, the energy to which the PL red shifted moved to higher energy at higher pressures (Figure 6), indicating that material

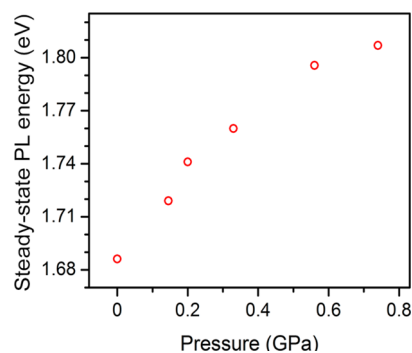


Figure 6. Pressure dependence of the energy to which the PL band asymptotes with light exposure for $(\text{MA})\text{Pb}(\text{Br}_{0.6}\text{I}_{0.4})_3$. Reproduced from ref 43.

compression does mitigate phase segregation, as anticipated. At a pressure of 0.9 GPa, when the perovskite is in its high-pressure phase, they saw no evidence of the PL red shift, suggesting that the Hoke effect is suppressed in the high-pressure β phase. Recognizing that commercial solar cells will not be operated under high pressure, Jaffe et al. suggest, based on previous work with AMnF_4 ($A = \text{Cs}, \text{Rb}, \text{K}$),⁵⁰ that similar effects may be realized through chemical pressure imposed through A-site substitution. Indeed, the enhanced stability against the Hoke effect observed in mixed-A-site perovskites^{41,42} may be due to the effects of chemical pressure.

Important to note for the aforementioned measurements modifying composition, morphology, and pressure is the intensity dependence of the Hoke effect. At sufficiently low excitation densities, even photounstable $\text{MAPb}(\text{Br}_x\text{I}_{1-x})_3$ films

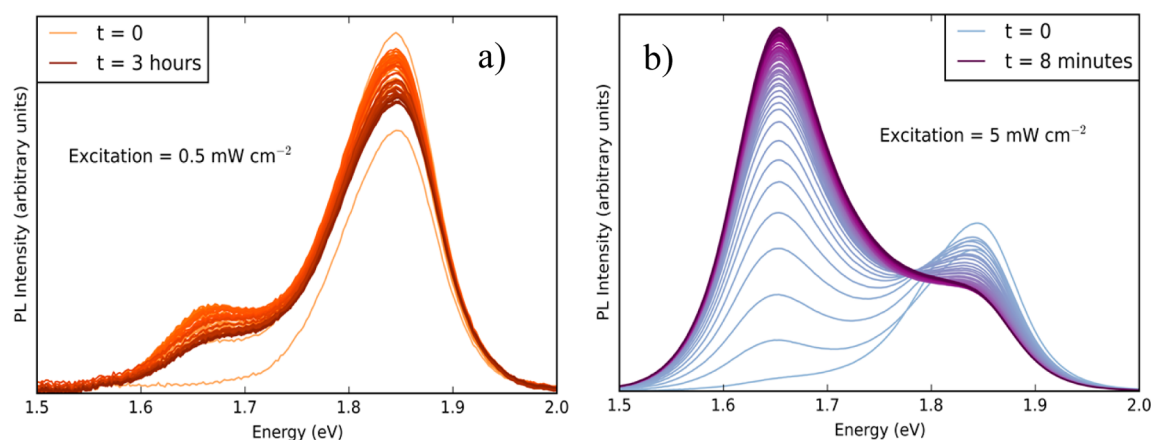


Figure 7. PL spectra of the same MAPb(Br_{0.4}I_{0.6})₃ film excited with (a) 0.5 mW/cm² (~1/200 sun) and (b) 5 mW/cm² (1/20 sun) light at 457 nm.

Table 1. Examples of Perovskites within a Given Range of Band Gaps, Reported Device Efficiencies, and Evaluation of Their Stability to Light-Induced Phase Segregation

band gap (eV)	material	device efficiency (%)	stable to phase segregation
<1.55	FAPbI ₃	17.4 ¹²	yes
	(FAPbI ₃) _{0.83} (MAPbBr ₃) _{0.17}	20.2 ⁵²	? ^a
1.55–1.65	MAPbI ₃	19.7 ¹¹	yes
	FA _{0.9} Cs _{0.1} PbI ₃	16.5 ⁵³	yes
	Cs _{0.05} (MA _{0.17} FA _{0.83}) _{0.95} Pb(I _{0.83} Br _{0.17}) ₃	21.1 ¹⁰	? ^a
1.65–1.75	FA _{0.83} Cs _{0.17} (I _{0.6} Br _{0.4}) ₃	17.1 ⁴¹	? ^a
	MAPbBr _{0.8} I _{2.2}	14.9 ⁴⁰	? ^a
1.8	MAPbI ₂ Br	11.0 ⁵⁴	no
1.9	CsPbBrI ₂	6.5 ⁴²	yes
2.3	MAPbBr ₃	8.3 ⁵⁵	yes
	CsPbBr ₃	6.2 ⁵⁶	yes

^aThe ? indicates that the material has shown evidence of stability under some conditions.

will remain mostly in a single phase (see Figure 7a). At such low excitation densities, the low carrier concentration may not be sufficient to promote halide segregation. However, we begin to observe the Hoke effect when increasing the excitation intensity over some material- and morphology-dependent critical threshold (see Figure 7b). This means that simply observing stable PL energy over time is insufficient to claim photostability; excitation must be at solar-relevant intensities to make such a claim as there may be an insufficient thermodynamic driving force and/or kinetic energy at low excitation densities. As the intensity dependence of the Hoke effect has not previously been well understood, many mixed-halide perovskites used in solar cells have not been tested for their stability to phase segregation. Table 1 organizes by band gap some of the most efficient perovskite solar absorbers and assesses their stability to the Hoke effect.

Data from Yang et al. suggest that exposure time is extremely important for determining the photostability.⁵¹ By varying repetition rates at constant average power in a pulsed laser and measuring the PL, they effectively manipulated the charge carrier concentration as a function of time in the perovskite. At low frequencies (≤ 500 Hz), when the perovskite sees a large number of carriers for a very short time, they observed only the original, higher-energy PL peak. However, as they increased the ratio of time that the perovskite spent in the presence of excited carriers to time spent without excited carriers by increasing the repetition rate, they observed a continuous shift of the PL peak position toward that of the lower-band-gap I-rich phase. At 1 MHz, the PL spectrum that they measured matched their continuous-wave

excitation spectrum, indicating that the perovskite had been populated by excited carriers long enough to drive and maintain the Hoke effect. Because the Hoke effect occurred at the lowest instantaneous power (highest repetition rate), we know that total average power is insufficient for determining stability to the Hoke effect and that excitation must be continuous to evaluate stability.

Future Opportunities. With a goal of achieving stable materials with a wide range of tunable band gaps, efforts to mitigate the Hoke effect have focused on compositional/structural changes as well as defect reduction. Several experimental and theory groups have shown that exchanging FA and/or Cs for MA, increasing the grain size, or changing the equilibrium defect concentrations or lattice stiffness (via external pressure) effectively limits the extent to which the Hoke effect occurs relative to MAPb(Br_xI_{1-x})₃.

Both theoretical and experimental findings provide guidelines for the development of future mixed-halide perovskites. On the basis of experimental evidence and supported by theory, we know that using FA or Cs instead of MA as the A-site cation significantly stabilizes the perovskite against the Hoke effect. Along these lines, other A-site cations as well as blends of A-site cations offer significant room for compositional exploration. Experiments also show that reducing defect concentration by improving crystallinity kinetically limits the Hoke effect. Larger grains and lower-vacancy concentrations reduce and may effectively eliminate phase segregation, and further, film optimization should continue to improve phase stability. Though it has not yet been proven experimentally, spatially improving compositional homogeneity in the parent film should also limit the Hoke effect. Increasing spatial homogeneity increases the

kinetic barrier for initiation of phase segregation and may slow or eliminate it entirely. Finally, recent efforts have been made to modify the perovskite's band gap for tandem solar cells by changing the B site,^{15,22} specifically focused on substituting Sn for Pb. However, the effects of interchanging the B-site cation on stability against the Hoke effect remain to be investigated. This substitution could prove to have significant impact on the thermodynamics and kinetics of mixed-halide systems. All of these modifications working in conjunction should lead to mixed-halide perovskites that show no signs of the Hoke effect at solar-relevant illumination intensities, paving the way for higher voltages to be realized from solar cells made with mixed-halide perovskite absorbers.

AUTHOR INFORMATION

Corresponding Authors

*E-mail: hemamala@stanford.edu (H.I.K.).

*E-mail: mmcgehee@stanford.edu (M.D.M.).

ORCID

Michael D. McGehee: 0000-0001-9609-9030

Notes

The authors declare no competing financial interest.

Biographies

Dan Slotcavage is a Ph.D. candidate in the Materials Science and Engineering Department at Stanford University whose research interests center around developing materials for sustainability. More specifically, Dan uses spectroscopic techniques to study hybrid perovskites and dynamic windows. He received his B.S. from the Pennsylvania State University.

Hemamala Karunadasa is an Assistant Professor in Chemistry at Stanford University. Her group synthesizes functional organic–inorganic hybrids with an emphasis on 2D and 3D hybrid perovskites. She received her A.B. from Princeton University and her Ph.D. from the University of California at Berkeley.

Mike McGehee is a Professor in the Materials Science and Engineering Department and a Senior Fellow of the Precourt Institute for Energy. His research interests are developing new materials for smart windows and solar cells. He received his undergraduate degree in physics from Princeton University and his Ph.D. degree in Materials Science from the University of California at Santa Barbara, where he did research on polymer lasers in the lab of Nobel Laureate Alan Heeger.

ACKNOWLEDGMENTS

This research was funded by the Global Climate and Energy Project (GCEP), the Sunshot NextGen III program (DE-EE0006707), and the National Science Foundation (DMR-1351538). D.J.S. acknowledges financial support of a Stanford Graduate Fellowship. We thank Eric Hoke for his continued feedback and early role in this project.

REFERENCES

- (1) Kojima, A.; Teshima, K.; Shirai, Y.; Miyasaka, T. Organometal Halide Perovskites as Visible-Light Sensitizers for Photovoltaic Cells. *J. Am. Chem. Soc.* **2009**, *131*, 6050–6051.
- (2) Walsh, A.; Scanlon, D. O.; Chen, S.; Gong, X. G.; Wei, S.-H. Self-Regulation Mechanism for Charged Point Defects in Hybrid Halide Perovskites. *Angew. Chem., Int. Ed.* **2015**, *54*, 1791–1794.
- (3) Yin, W.-J.; Shi, T.; Yan, Y. Unusual Defect Physics in CH₃NH₃PbI₃ Perovskite Solar Cell Absorber. *Appl. Phys. Lett.* **2014**, *104*, 063903.
- (4) Steirer, K. X.; Schulz, P.; Teeter, G.; Stevanovic, V.; Yang, M.; Zhu, K.; Berry, J. J. Defect Tolerance in Methylammonium Lead Triiodide Perovskite. *ACS Energy Lett.* **2016**, *1*, 360–366.

(5) De Wolf, S.; Holovsky, J.; Moon, S.; Löper, P.; Niesen, B.; Ledinsky, M.; Haug, F.; Yum, J.; Ballif, C. Organometallic Halide Perovskites: Sharp Optical Absorption Edge and Its Relation to Photovoltaic Performance. *J. Phys. Chem. Lett.* **2014**, *5*, 1035–1039.

(6) Stranks, S. D.; Eperon, G. E.; Grancini, G.; Menelaou, C.; Alcocer, M. J. P.; Leijtens, T.; Herz, L. M.; Petrozza, A.; Snaith, H. J. Electron-Hole Diffusion Lengths Exceeding 1 Micrometer in an Organometal Trihalide Perovskite Absorber. *Science (Washington, DC, U. S.)* **2013**, *342*, 341–344.

(7) Yang, Y.; Yan, Y.; Yang, M.; Choi, S.; Zhu, K.; Luther, J. M.; Beard, M. C. Low Surface Recombination Velocity in Solution-Grown CH₃NH₃PbBr₃ Perovskite Single Crystal. *Nat. Commun.* **2015**, *6*, 7961.

(8) Stranks, S. D.; Snaith, H. J. Metal-Halide Perovskites for Photovoltaic and Light-Emitting Devices. *Nat. Nanotechnol.* **2015**, *10*, 391–402.

(9) Veldhuis, S. A.; Boix, P. P.; Yantara, N.; Li, M.; Sum, T. C.; Mathews, N.; Mhaisalkar, S. G. Perovskite Materials for Light-Emitting Diodes and Lasers. *Adv. Mater.* **2016**, *28*, 6804–6834.

(10) Saliba, M.; Matsui, T.; Seo, J.-Y.; Domanski, K.; Correa-Baena, J.-P.; Nazeeruddin, M. K.; Zakeeruddin, S. M.; Tress, W.; Abate, A.; Hagfeldt, A.; et al. Cesium-Containing Triple Cation Perovskite Solar Cells: Improved Stability, Reproducibility and High Efficiency. *Energy Environ. Sci.* **2016**, *9*, 1989–1997.

(11) Ahn, N.; Son, D.-Y.; Jang, I.-H.; Kang, S. M.; Choi, M.; Park, N.-G. Highly Reproducible Perovskite Solar Cells with Average Efficiency of 18.3% and Best Efficiency of 19.7% Fabricated via Lewis Base Adduct of Lead(II) Iodide. *J. Am. Chem. Soc.* **2015**, *137*, 8696–8699.

(12) Zhou, Y.; Yang, M.; Pang, S.; Zhu, K.; Padture, N. P. Exceptional Morphology-Preserving Evolution of Formamidinium Lead Triiodide Perovskite Thin Films via Organic-Cation Displacement. *J. Am. Chem. Soc.* **2016**, *138*, 5535–5538.

(13) Jeon, N. J.; Noh, J. H.; Yang, W. S.; Kim, Y. C.; Ryu, S.; Seo, J.; Seok, S. I. Compositional Engineering of Perovskite Materials for High-Performance Solar Cells. *Nature* **2015**, *517*, 476–480.

(14) Bush, K. A.; Bailie, C. D.; Chen, Y.; Bowring, A. R.; Wang, W.; Ma, W.; Leijtens, T.; Moghadam, F.; McGehee, M. D. Thermal and Environmental Stability of Semi-Transparent Perovskite Solar Cells for Tandems Enabled by a Solution-Processed Nanoparticle Buffer Layer and Sputtered ITO Electrode. *Adv. Mater.* **2016**, *28*, 3937–3943.

(15) Eperon, G. E.; Leijtens, T.; Bush, K. A.; Prasanna, R.; Green, T.; Wang, J. T.-W.; McMeekin, D. P.; Volonakis, G.; Milot, R. L.; May, R.; et al. Perovskite-Perovskite Tandem Photovoltaics with Optimized Bandgaps. *Science (Washington, DC, U. S.)* **2016**, *351*, 1–10.

(16) Kranz, L.; Abate, A.; Feurer, T.; Fu, F.; Avancini, E.; Löckinger, J.; Reinhard, P.; Zakeeruddin, S. M.; Grätzel, M.; Buecheler, S.; et al. High-Efficiency Polycrystalline Thin Film Tandem Solar Cells. *J. Phys. Chem. Lett.* **2015**, *6*, 2676–2681.

(17) Chen, B.; Bai, Y.; Yu, Z.; Li, T.; Zheng, X.; Dong, Q.; Shen, L.; Boccad, M.; Gruverman, A.; Holman, Z.; et al. Efficient Semi-transparent Perovskite Solar Cells for 23.0%-Efficiency Perovskite/Silicon Four-Terminal Tandem Cells. *Adv. Energy Mater.* **2016**, *6*, 1601128.

(18) Mailoa, J. P.; Bailie, C. D.; Johlin, E. C.; Hoke, E. T.; Akey, A. J.; Nguyen, W. H.; McGehee, M. D.; Buonassisi, T. A 2-Terminal Perovskite/Silicon Multijunction Solar Cell Enabled by a Silicon Tunnel Junction. *Appl. Phys. Lett.* **2015**, *106*, 121105.

(19) Bailie, C. D.; Christoforo, M. G.; Mailoa, J. P.; Bowring, A. R.; Unger, E. L.; Nguyen, W. H.; Burschka, J.; Pellet, N.; Lee, J. Z.; Grätzel, M.; et al. Semi-Transparent Perovskite Solar Cells for Tandems with Silicon and CIGS. *Energy Environ. Sci.* **2015**, *8*, 956–963.

(20) Löper, P.; Moon, S.-J.; Martin de Nicolas, S.; Niesen, B.; Ledinsky, M.; Nicolay, S.; Bailat, J.; Yum, J.-H.; De Wolf, S.; Ballif, C. Organic–inorganic Halide Perovskite/crystalline Silicon Four-Terminal Tandem Solar Cells. *Phys. Chem. Chem. Phys.* **2015**, *17*, 1619–1629.

(21) Albrecht, S.; Saliba, M.; Correa Baena, J. P.; et al. Monolithic Perovskite/silicon-Heterojunction Tandem Solar Cells Processed at Low Temperature. *Energy Environ. Sci.* **2016**, *9*, 81–88.

- (22) Yang, Z.; Rajagopal, A.; Chueh, C.; Jo, S. B.; Liu, B.; Zhao, T.; Jen, A. K.-Y. Stable Low-Bandgap Pb-Sn Binary Perovskites for Tandem Solar Cells. *Adv. Mater.* **2016**, *28*, 8990–8997.
- (23) Coutts, T. J.; Emery, K. A.; Ward, J. S. Modeled Performance of Polycrystalline Thin-Film Tandem Solar Cells. *Prog. Photovoltaics* **2002**, *10*, 195–203.
- (24) Yi, C.; Luo, J.; Meloni, S.; Boziki, A.; Ashari-Astani, N.; Grätzel, C.; Zakeeruddin, S. M.; Röthlisberger, U.; Grätzel, M. Entropic Stabilization of Mixed A-Cation ABX₃ Metal Halide Perovskites for High Performance Perovskite Solar Cells. *Energy Environ. Sci.* **2016**, *9*, 656–662.
- (25) Noh, J. H.; Im, S. H.; Heo, J. H.; Mandal, T. N.; Seok, S. I. Chemical Management for Colorful, Efficient, and Stable Inorganic-Organic Hybrid Nanostructured Solar Cells. *Nano Lett.* **2013**, *13*, 1764–1769.
- (26) Hoke, E. T.; Slotcavage, D. J.; Dohner, E. R.; Bowring, A. R.; Karunadasa, H. I.; McGehee, M. D. Reversible Photo-Induced Trap Formation in Mixed-Halide Hybrid Perovskites for Photovoltaics. *Chem. Sci.* **2015**, *6*, 613–617.
- (27) Tanaka, K.; Takahashi, T.; Ban, T.; Kondo, T.; Uchida, K.; Miura, N. Comparative Study on the Excitons in Lead-Halide-Based Perovskite-Type Crystals CH₃NH₃PbBr₃ CH₃NH₃PbI₃. *Solid State Commun.* **2003**, *127*, 619–623.
- (28) Xing, G.; Mathews, N.; Sun, S.; Lim, S. S.; Lam, Y. M.; Grätzel, M.; Mhaisalkar, S.; Sum, T. C. Long-Range Balanced Electron- and Hole-Transport Lengths in Organic-Inorganic CH₃NH₃PbI₃. *Science (Washington, DC, U. S.)* **2013**, *342*, 344–347.
- (29) Shi, D.; Adinolfi, V.; Comin, R.; Yuan, M.; Alarousu, E.; Buin, A.; Chen, Y.; Hoogland, S.; Rothenberger, A.; Katsiev, K.; et al. Low Trap-State Density and Long Carrier Diffusion in Organolead Trihalide Perovskite Single Crystals. *Science (Washington, DC, U. S.)* **2015**, *347*, 519–522.
- (30) Kuku, T. Structure and Ionic Conductivity of CuCdCl₃. *Solid State Ionics* **1987**, *25*, 105–108.
- (31) Kuku, T.; Salau, A. Electrical Conductivity of CuSnI₃, CuPbI₃, and KPbI₃. *Solid State Ionics* **1987**, *25*, 1–7.
- (32) Kuku, T. Ionic Transport and Galvanic Cell Discharge Characteristics of CuPbI₃ Thin Films. *Thin Solid Films* **1998**, *325*, 246–250.
- (33) Mizusaki, J.; Arai, K.; Fueki, K. Ionic Conduction of the Perovskite-Type Halides. *Solid State Ionics* **1983**, *11*, 203–211.
- (34) Yoon, S. J.; Draguta, S.; Manser, J. S.; Sharia, O.; Schneider, W. F.; Kuno, M.; Kamat, P. V. Tracking Iodide and Bromide Ion Segregation in Mixed Halide Lead Perovskites during Photoirradiation. *ACS Energy Lett.* **2016**, *1*, 290–296.
- (35) Bischak, C. G.; Hetherington, C. L.; Wu, H.; Aloni, S.; Ogletree, D. F.; Limmer, D. T.; Ginsberg, N. S. Origin of Reversible Photo-Induced Phase Separation in Hybrid Perovskites. *arXiv* **2016**, 1–6.
- (36) Brivio, F.; Caetano, C.; Walsh, A. Thermodynamic Origin of Photoinstability in the CH₃NH₃ Pb(I–X Br X)₃ Hybrid Halide Perovskite Alloy. *J. Phys. Chem. Lett.* **2016**, *7*, 1083–1087.
- (37) Wright, A. D.; Verdi, C.; Milot, R. L.; Eperon, G. E.; Pérez-Osorio, M. A.; Snaith, H. J.; Giustino, F.; Johnston, M. B.; Herz, L. M. Electron-phonon Coupling in Hybrid Lead Halide Perovskites. *Nat. Commun.* **2016**, DOI: 10.1038/ncomms11755.
- (38) Wehrenfennig, C.; Liu, M.; Snaith, H. J.; Johnston, M. B.; Herz, L. M. Homogeneous Emission Line Broadening in the Organo Lead Halide Perovskite CH₃NH₃PbI_{3-x}Cl_x. *J. Phys. Chem. Lett.* **2014**, *5*, 1300–1306.
- (39) Neukirch, A. J.; Nie, W.; Blancon, J.-C.; Appavoo, K.; Tsai, H.; Sfeir, M. Y.; Katan, C.; Pedesseau, L.; Even, J.; Crochet, J. J.; et al. Polaron Stabilization by Cooperative Lattice Distortion and Cation Rotations in Hybrid Perovskite Materials. *Nano Lett.* **2016**, *16*, 3809–3816.
- (40) Hu, M.; Bi, C.; Yuan, Y.; Bai, Y.; Huang, J. Stabilized Wide Bandgap MAPbBr₃ X I_{3-x} Perovskite by Enhanced Grain Size and Improved Crystallinity. *Adv. Sci.* **2016**, *3*, 1500301.
- (41) McMeekin, D. P.; Sadoughi, G.; Rehman, W.; Eperon, G. E.; Saliba, M.; Horantner, M. T.; Haghighirad, A.; Sakai, N.; Korte, L.; Rech, B.; et al. A Mixed-Cation Lead Mixed-Halide Perovskite Absorber for Tandem Solar Cells. *Science (Washington, DC, U. S.)* **2016**, *351*, 151–155.
- (42) Beal, R. E.; Slotcavage, D. J.; Leijtens, T.; Bowring, A. R.; Belisle, R. A.; Nguyen, W. H.; Burkhard, G. F.; Hoke, E. T.; McGehee, M. D. Cesium Lead Halide Perovskites with Improved Stability for Tandem Solar Cells. *J. Phys. Chem. Lett.* **2016**, *7*, 746–751.
- (43) Jaffe, A.; Lin, Y.; Beavers, C. M.; Voss, J.; Mao, W. L.; Karunadasa, H. I. High-Pressure Single-Crystal Structures of 3D Lead-Halide Hybrid Perovskites and Pressure Effects on Their Electronic and Optical Properties. *ACS Cent. Sci.* **2016**, *2*, 201–209.
- (44) Verwey, J. F. F.; Schoonman, J. Crystal Growth, Ionic Conductivity, and Photolysis of Pure and Impurity-Doped Lead Bromide Single Crystals. *Physica* **1967**, *35*, 386–394.
- (45) Eames, C.; Frost, J. M.; Barnes, P. R. F.; O'Regan, B. C.; Walsh, A.; Islam, M. S. Ionic Transport in Hybrid Lead Iodide Perovskite Solar Cells. *Nat. Commun.* **2015**, *6*, 7497.
- (46) Yun, J. S.; Seidel, J.; Kim, J.; Soufiani, A. M.; Huang, S.; Lau, J.; Jeon, N. J.; Seok, S. I.; Green, M. A.; Ho-Baillie, A. Critical Role of Grain Boundaries for Ion Migration in Formamidinium and Methylammonium Lead Halide Perovskite Solar Cells. *Adv. Energy Mater.* **2016**, *6*, 1600330.
- (47) Sutter-Fella, C. M.; Li, Y.; Amani, M.; Ager, J. W.; Toma, F. M.; Yablonovitch, E.; Sharp, I. D.; Javey, A. High Photoluminescence Quantum Yield in Band Gap Tunable Bromide Containing Mixed Halide Perovskites. *Nano Lett.* **2016**, *16*, 800–806.
- (48) Azpiroz, J. M.; Mosconi, E.; Bisquert, J.; De Angelis, F. Defect Migration in Methylammonium Lead Iodide and Its Role in Perovskite Solar Cell Operation. *Energy Environ. Sci.* **2015**, *8*, 2118–2127.
- (49) Haruyama, J.; Sodeyama, K.; Han, L.; Tateyama, Y. First-Principles Study of Ion Diffusion in Perovskite Solar Cell Sensitizers. *J. Am. Chem. Soc.* **2015**, *137*, 10048–10051.
- (50) Morón, M. C.; Palacio, F.; Clark, S. M. Pressure-Induced Structural Phase Transitions in the A MnF₄ Series (A = Cs, Rb, K) Studied by Synchrotron X-Ray Powder Diffraction: Correlation between Hydrostatic and Chemical Pressure. *Phys. Rev. B: Condens. Matter Mater. Phys.* **1996**, *54*, 7052–7061.
- (51) Yang, X.; Yan, X.; Wang, W.; Zhu, X.; Li, H.; Ma, W.; Sheng, C. X. Light Induced Metastable Modification of Optical Properties in CH₃NH₃PbI_{3-x}Br_x Perovskite Films: Two-Step Mechanism. *Org. Electron.* **2016**, *34*, 79–83.
- (52) Yang, W. S.; Noh, J. H.; Jeon, N. J.; Kim, Y. C.; Ryu, S.; Seo, J.; Seok, S. I. High-Performance Photovoltaic Perovskite Layers Fabricated through Intramolecular Exchange. *Science (Washington, DC, U. S.)* **2015**, *348*, 1234–1237.
- (53) Lee, J.; Kim, D.-H.; Kim, H.; Seo, S.; Cho, S. M.; Park, N. Formamidinium and Cesium Hybridization for Photo- and Moisture-Stable Perovskite Solar Cell. *Adv. Energy Mater.* **2015**, *5*, 1501310.
- (54) Cao, K.; Cui, J.; Zhang, H.; Li, H.; Song, J.; Shen, Y.; Cheng, Y.; Wang, M. Efficient Mesoscopic Perovskite Solar Cells Based on the CH₃NH₃PbI₃Br Light Absorber. *J. Mater. Chem. A* **2015**, *3*, 9116–9122.
- (55) Sheng, R.; Ho-Baillie, A.; Huang, S.; Chen, S.; Wen, X.; Hao, X.; Green, M. A. Methylammonium Lead Bromide Perovskite-Based Solar Cells by Vapor-Assisted Deposition. *J. Phys. Chem. C* **2015**, *119*, 3545–3549.
- (56) Kulbak, M.; Gupta, S.; Kedem, N.; Levine, I.; Bendikov, T.; Hodes, G.; Cahen, D. Cesium Enhances Long-Term Stability of Lead Bromide Perovskite-Based Solar Cells. *J. Phys. Chem. Lett.* **2016**, *7*, 167–172.